DOI 10.5162/IMCS2012/P1.7.8

Direct fabrication of $La_{0.7}Sr_{0.3}FeO_3$ hollow nanofibers by electrospinning and their gas sensing properties

Peng-Jun Yao[1,2], Jing Wang[1], Hai-ying Du[1,3], Lin Zhao[1]*
[1] School of Electronic Science and Technology, Dalian University of Technology, Dalian 116023, PR China, E-mail address: wangjing@dlut.edu.cn
[2] School of Educational Technology, Shenyang Normal University, Shenyang 110034, PR China
[3] Department of Electromechanical Engineering & Information, Dalian Nationalities University, Dalian 116600, China

Abstract:
$La_{0.7}Sr_{0.3}FeO_3$ hollow nanofibers are prepared by a facile single capillary electrospinning and calcination process. The hollow nanofibers are characterized by Scanning electron microscopy, Transmission electron microscopy and X-ray diffraction. The results indicate that the outer diameters of the hollow nanofibres range in 80-200 nm, and shell thickness are about 20 nm. Formaldehyde gas sensing properties are carried out in the concentration range of 0.1-100 ppm at the optimum operating temperature 240°C. The response and recovery times, and the cross-response to ethanol, toluene, benzene, acetone, methanol, ammonia are measured.

Key words: hollow nanofibers, electrospinning, $La_{0.7}Sr_{0.3}FeO_3$, gas sensing

Introduction

Recently, one-dimensional nanostructures such as nanowires, nanofibers, nanobelts, nanotubes and nanorods have been extensively studied due to their unique properties and novel applications for catalysts, batteries and gas sensors [1-3]. Nanofibers-based gas sensors have attracted much attention owing to the characteristics of large surface-to-volume and high length-to-diameter ratios, which is believed to contribute to the high sensitivity [4, 5]. In comparison with solid nanofibers, hollow nanofibers provide enhanced surface activity such as high surface reactions and fast diffusion because of high surface permeability and low-density, providing percolation paths and allowing gas to penetrate into the sensing layers [6, 7].

Coaxial electrospinning has been employed to prepare hollow nanofibers [8]. However, the technique cannot overcome some problems, such as how to select a suitable inner solvent and how to accurately control electrospinning parameters [9]. To solve these shortcomings, a single capillary electrospinning has been applied in fabricating hollow nanofibers. SnO_2 [10], CuO [11] and ZnO [12] hollow nanofibers have been fabricated by using the method.

In this report, we synthesize $La_{0.7}Sr_{0.3}FeO_3$ hollow nanofibers by employing the facile single capillary electrospinning followed by a heat treatment. And the formaldehyde (HCHO) gas sensing properties based on the hollow nanofibers are investigated.

Experimental

In a typical process, 0.1551 g $La(NO_3)_3 \cdot 6H_2O$, 0.0318 g $Sr(NO_3)_2$ and 0.2020 g $Fe(NO_3)_3 \cdot 9H_2O$ were dissolved in a mixture of 5 ml ethanol, 2.7 ml N,N-dimethylformamide (DMF) and 2 ml deionized water as solvent to form a homogeneous solution. Subsequently, 0.7776 g poly(viny pyrrolidone) (PVP) was added into the solution. The mixture was magnetically stirred at room temperature for 9 h. Then the solution was loaded into a glass syringe and electrospun by applying 20 kV at an electrode distance of 10 cm. The as-spun composite nanofibers were calcined at 500°C for 6 h with a heating rate of 1°C/min to obtain $La_{0.7}Sr_{0.3}FeO_3$ hollow nanofibers.

The as-synthesized sample was mixed with deionized water to form a paste. The paste was coated on a ceramic tube on which a pair of gold electrodes was previously printed. Then a 30 Ω Ni-Cr heating wire was inserted in the tube to form a side-heated gas sensor [13]. A heating voltage was applied on the heating wire to provide the operating temperature.

Gas sensing properties were measured by a static state distribution. The sensor was put into

a 50 L chamber. Saturated target vapor was injected into the test chamber by a micro-injector through a rubber plug. When the response reached a constant value, the front door of the chamber was opened to recover in air. The sensor's resistance was measured by using a conventional circuit described in the literature [14]. An external resistor was used to connect with the sensor in series at a circuit voltage of 10 V. The resistance of the gas sensor in target gas was calculated as the follows: $R_S = R_L \times (10-V_L)/V_L$, where R_S, R_L and V_L are the resistance of the sensor, the resistance of the reference resistor and the measured voltage, respectively. A computer monitored and recoded the change of voltage signal V_L by an A/D data acquisition card. The response of the gas sensor was defined as $R=R_g/R_a$, where R_g and R_a represented the resistance of the gas sensor in target gas and in air, respectively. The response time and recovery time were defined as the time taken by the sensor to obtain 90% of the total resistance change in the case of desorption and desorption, respectively.

Scanning electron microscopy (SEM) pictures were examined on a FEI QUANTA 200F (United States) microscope equipped with energy dispersive X-ray (EDX) spectroscopy. X-ray diffraction (XRD) data were measured by X-ray diffractometer on Shimadzu XRD-6000 (Japan) with Cu Kα (1.5406 Å). Crystallite size was evaluated by Scherror formula of $0.9\lambda/\beta\cos\theta$, where, λ is the wavelength of the target Cu Kα 1.5406 Å, β is the full width at half maximum. Transmission electron microscopy (TEM) image was performed to obtain the size and structure by Tecnai G220 S-Twin (United States) instrument.

Results and Discussion

Fig. 1a displays the SEM pictures of the as-synthesized $La_{0.7}Sr_{0.3}FeO_3$ nanofibers. The sample is highly dominated by the nanofibers with length of several ten micrometers and diameters ranging from 80 to 200 nm. It can be observed from the inset in Fig. 1a that the cross sections of these nanofibers are hollow. And the shell thickness is about 20 nm. Fig. 1b shows the TEM of an individual nanofiber, which indicates a typical characteristic of the nanofiber and confirms the hollow structure. The diameter of the hollow nanofiber in Fig. 1b is about 80 nm and the shell thickness is 20 nm. The surface of the hollow nanofiber is rough and porous, which consists of nanoparticles with average size of 25 nm.

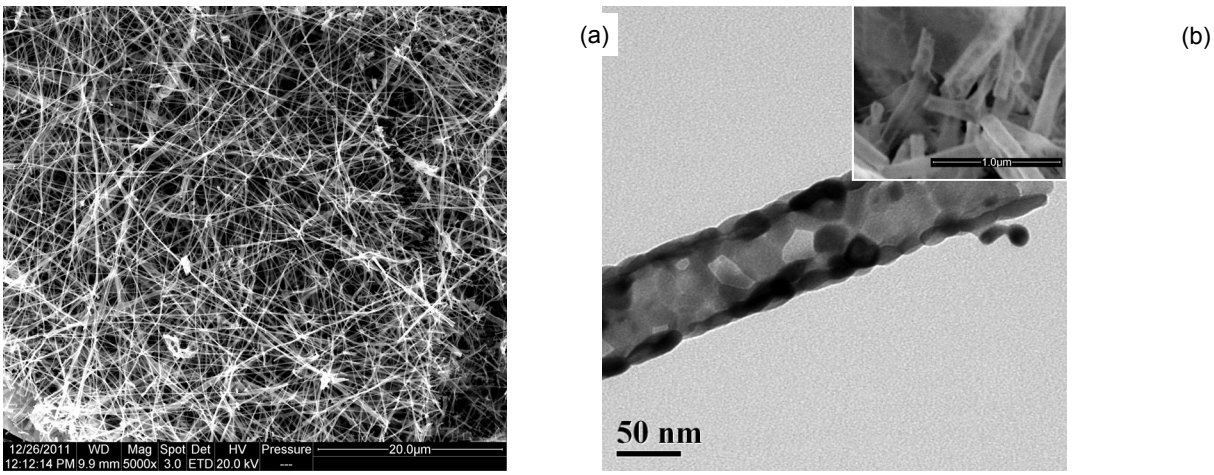

Fig. 1. (a) SEM and (b) TEM images of $La_{0.7}Sr_{0.3}FeO_3$ hollow nanofibers, the inset shows hollow nanofibers at the high-magnification.

Fig. 2a shows XRD patterns of the as-synthesized $La_{0.7}Sr_{0.3}FeO_3$ hollow nanofibers. The prominent peaks corresponding to (020), (220) and (024) crystal lattice planes and all other minor peaks coincide with corresponding phase of orthorhombic perovskite structure of $La_{0.7}Sr_{0.3}FeO_3$ with pbnm (62) space group provided by JCPDS 89-1269. The calculated crystallite size is around 20 nm, which is consistent with the results of TEM shown in Fig. Fig. 1b. The EDX pattern shown in Fig. 2b reveals that the nanofibers are composed of La, Sr, Fe and O. The C peak in the spectrum is attributed to the electric latex of the SEM sample holder.

Fig. 3 shows the resistance change of the $La_{0.7}Sr_{0.3}FeO_3$ hollow nanofibers based sensor to 20 ppm HCHO versus different operating temperature. The resistance of the sensor increases when exposed in HCHO, which indicates that $La_{0.7}Sr_{0.3}FeO_3$ hollow nanofibers

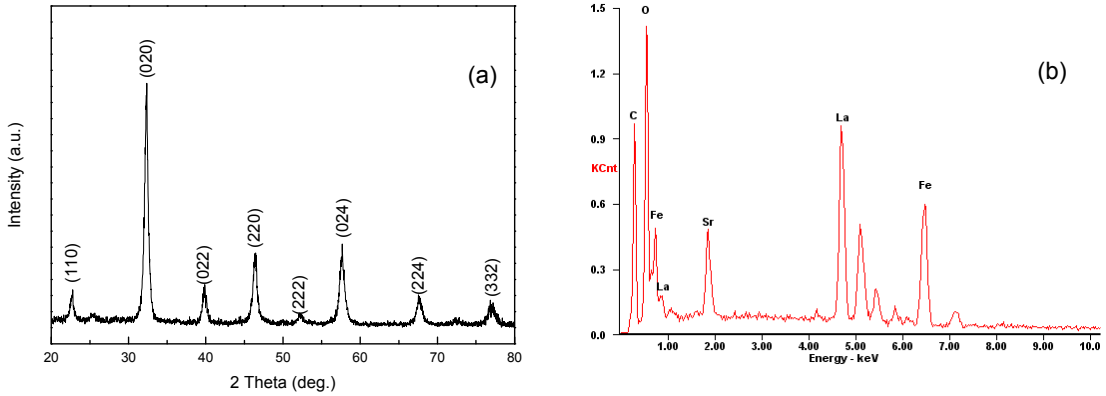

Fig. 2. (a) XRD and (b) EDX patterns of $La_{0.7}Sr_{0.3}FeO_3$ hollow nanofibers.

shows p-type behavior. The gas sensor responses quickly to HCHO gas at all the operating temperatures. However, the sensor cannot recover to initial resistance at 200 and 220°C. The sensor can recover to initial value at temperatures above 240°C. In this case, 240°C was selected as the optimum operating temperature. At this operating temperature, the response and recovery times of the sensor to 20 ppm HCHO are 220 s and 100 s, respectively. The response and recovery times are longer than other HCHO gas sensors, which may due to the testing method. In our experiments, the statics state distribution in a 50 L chamber was used. The vaporization of the HCHO liquid and a slow gas exchange in the test chamber would cause the longer response and recovery times.

The response of the gas sensor to different concentrations of HCHO at 240°C is shown in Fig. 4. The response is about 1.5, 2.1, 2.3, 8.2, 12.2, 21, 25.8, 31.1, 43.2 and 47.8 to 0.1, 0.5, 1, 5, 10, 20, 30, 40, 50 and 100 ppm, respectively. Below 1 ppm, the response slowly increases as HCHO concentration increases. Above 1 ppm, the response increases rapidly with increasing HCHO concentration. Finnally the gas sensor reaches saturation at 100 ppm.

The response of the sensor to 20 ppm ethanol, toluene, benzene, acetone, methanol, ammonia and HCHO at the operating temperature of 240°C was measured. It can be seen from Fig. 5 that the sensor is sensitive to ethanol, acetone, methanol and HCHO, but is obviously insensitive to toluene, benzene and ammonia. Thus, for the $La_{0.7}Sr_{0.3}FeO_3$ hollow nanofibers-based gas sensor, ethanol, acetone and methanol are the main interference gases. The problem of cress-sensitivity will be solved by using pattern recognition.

As is well known, semiconductor oxides adsorb the oxygen molecule on the surface to generate chemisorbed species (O_2, O^{2-}, O^-). When exposed in HCHO, the chemisorbed oxygen species adsorbed on the surface of the $La_{0.7}Sr_{0.3}FeO_3$ hollow nanofibers react with HCHO. The products could be formic acid (CHOOH) and/or water and CO_2 [14]. Both of the reactions release electrons. The released electrons are compensated with the holes of *p*-type $La_{0.7}Sr_{0.3}FeO_3$, leading to the decreasing of

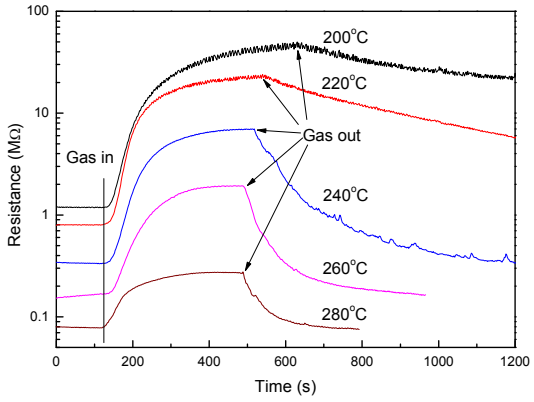

Fig. 3. The resistance change of the sensor to 20 ppm HCHO at different operating temperatures.

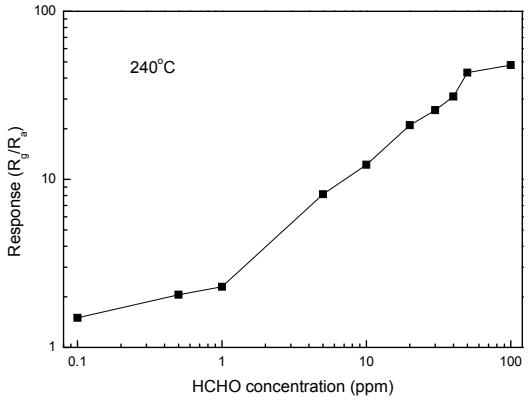

Fig. 4. The gas sensor responses as a function of HCHO concentration.

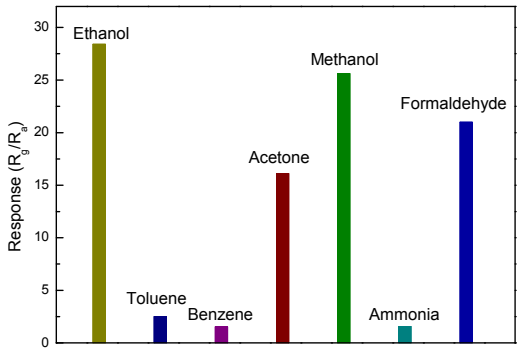

Fig. 5. The gas sensor responses as a function of HCHO concentration.

the conductivity of the material. As a result, the resistance of the sensor will increase. Hollow structure has the larger surface area, which will increase the number of active adsorption centers. In our case, $La_{0.7}Sr_{0.3}FeO_3$ hollow nanofibers have rough porous surface, which make the inner surface accessible and provide more gas channels. HCHO molecule can reach not only the outer but also the inner surface. Then the gas transport properties are improved, which will also improve the response.

Conclusions

In summary, $La_{0.7}Sr_{0.3}FeO_3$ hollow nanofibers are fabricated by electrospinning method. The length of the hollow nanofibers is several ten micrometers, and diameter is in the range of 80-200 nm. The sensor fabricated from these hollow fibers exhibits excellent HCHO sensing properties at 240°C. The gas sensor can detect as low as 0.1 ppm HCHO. Ethanol, acetone and methanol are the main interference gases of the sensor. Finally, the gas sensing mechanism is discussed. The rough porous surface of the hollow nanofibers helps to improve the response.

Acknowledgements

This subject was supported by the National Natural Science Foundation of China (61176068, 61131004 and 61001054).

References

[1] S. J. Guo, S. Zhang, X. L. Sun, S. H. Sun, Synthesis of Ultrathin FePtPd Nanowires and Their Use as Catalysts for Methanol Oxidation Reaction, *J. Am. Chem. Soc.* 133, 15354-15357 (2011); doi: 10.1021/ja207308b

[2] M. H. Park, Y. H. Cho, K. Kim, J. Kim, M. Liu, J. Cho, Germanium Nanotubes Prepared by Using the Kirkendall Effect as Anodes for High-Rate Lithium Batteries, *Angew. Chem.* 123, 9821-9824 (2011); doi: 10.1002/ange.201103062

[3] J. A. Park, J. Moon, S. J. Lee, S. H. Kim, H. Y. Chu, T. Zyung, SnO_2-ZnO Hybrid Nanofibers-based Highly Sensitive Nitrogen Dioxides Sensor, *Sens. Actuators B* 145, 592-595 (2010); doi: http://dx .doi.org/10.1016/j.snb.2009.11.023

[4] W. Wang, H. M. Huang, Z. Y. Li, H. N. Zhang, Y. Wang, W. Zheng, C. Wang, Zinc Oxide Nanofiber Gas Sensors Via Electrospinning, J. Am. Ceram. Soc. 91, 3817–3819 (2008), doi: 10.1111/j.1551-2916.2008.02765.x

[5] Y. Zhang, X. L. He, J. P. Li, Z. J. Miao, F. Huang, Fabrication and Ethanol-sensing Properties of Micro Gas Sensor Based on Electrospun SnO_2 Nanofibers, *Sens. Actuator B,* 132, 67–73 (2008); doi: http://dx.doi.org/10.1016/j.snb.2008.01.006

[6] J.H. Lee, Gas Sensors Using Hierarchical and Hollow Oxide Nanostructures: Overview, *Sens. Actuator B* 140, 319–336 (2009); doi: http://dx.doi.org/10.1016/j.snb.2009.04.026

[7] P.C. Chen, G. Shen, C. Zhou, Chemical Sensors and Electronic Noses Based on 1-D Metal Oxide Nanostructures, *IEEE Trans. Nanotechnol.* 7, 668–682 (2008); doi: 10.1109/TNANO.2008. 2006273

[8] D. Li, Y. N. Xia, Direct Fabrication of Composite and Ceramic Hollow Nanofibers by Electrospinning, Nano Lett, 4, 933-938 (2004); doi: 10.1021/nl049590f

[9] Z. Y. Zhang, X. H. Li, C. H. Wang, L. M. Wei, Y. C. Liu, C. L. Shao, ZnO Hollow Nanofibers: Fabrication from Facile Single Capillary Electrospinning and Applications in Gas Sensors, J. Phys. Chem. C 113, 19397-19403 (2009); doi: 10.1021/jp9070373

[10] N. G. Cho, D. J. Yang, M. J. Jin, H. G. Kim, H. L. Tuller, I. D. Kim, Highly sensitive SnO_2 hollow nanofiber-based NO_2 gas sensors, *Sens. Actuator B* 160, 1468-1472 (2011); doi:10.1016/j.snb.2011.07.035

[11] H. F. Xiang, Y. H. Long, X. L. Yu, X. L. Zhang, N. Zhao, J. Xu, A novel and facile method to prepare porous hollow CuO and Cu nanofibers based on electrospinning, CrystEngComm 13, 4856-4860 (2011); doi: 10.1039/C0CE00980F

[12] S. H. Wei, M. H. Zhou, W. P. Du, Improved acetone sensing properties of ZnO hollow nanofibers by single capillary electrospinning, *Sens. Actuator B* 160, 753-759 (2011); doi: 10.1016/j.snb.2011.08.059

[13] J. Wang, L. Liu, S. Y. Cong, J. Q. Qi, B. K. Xu, An enrichment method to detect low concentration formaldehyde, *Sens. Actuator B* 134, 1010–1015 (2008); doi: http://dx.doi.org/10.1016/j.snb.2008. 07. 010

[14] P.J. Yao, J. Wang, H. Y. Du, J. Q. Qi, Synthesis, characterization and formaldehyde gas sensitivity of $La_{0.7}Sr_{0.3}FeO_3$ nanoparticles assembled nanowires, *Mater. Chem. Phys.* (2012), doi: 10.1016/j.matchemphys.2012.02.029